Stress Evolution and Fault Interactions before and after the 2008 Great Wenchuan Earthquake

Gang Luo and Mian Liu

Department of Geological Sciences, University of Missouri, Columbia, MO, 65211 (Email: glk82@mizzou.edu)

INTRODUCTION

The 12 May 2008 Wenchuan earthquake (Mw 7.9) ruptured more than 300 km of the Longmen Shan fault, killing ~90,000 people and devastating many cities in the Sichuan province, China. Here we explore stress evolution before and after the great Wenchuan earthquake and fault interactions in eastern Tibet using a 3-D viscoelasto-plastic finite element model. Our results of the coseismic Coulomb stress changes are similar to previous studies, but the net results are significantly different when numerous large earthquakes in the region are included in the model. In particular, we found higher Coulomb stress on the eastern Kunlun fault and the southern Longmen Shan fault, but lower stress on southern segments of the Xianshuihe fault. Furthermore, we found that locking on the Xianshuihe fault can increase tectonic loading on the Longmen Shan fault and other faults in eastern Tibet at a rate up to ~50 Pa/yr.

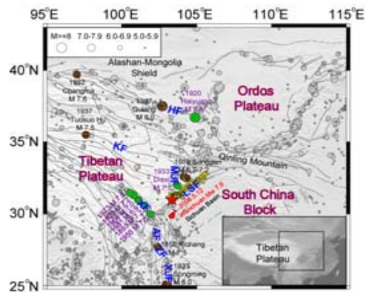

Fig. 1. Faults and seismicity in the eastern Tibetan Plateau and its neighboring region. Yellow circles shows aftershocks of the Wenchuan earthquake ending on 8/22/2008 (CENC, 2008). Green circles are big historic earthquakes modeled in this study. LSF: Longmen Shan fault; MJF: Min Jiang fault; KF: Kunlun fault; HF: Haiyuan fault; XF: Xianshuihe fault; AF: Anninghe fault; ZF: Zemuhe fault; XJF: Xiaojiang fault; W: Wenchuan-Maowen fault; Y: Yingxiu-Beichuan fault; G: Guanxian-Anxian fault.

FINITE ELEMENT MODEL

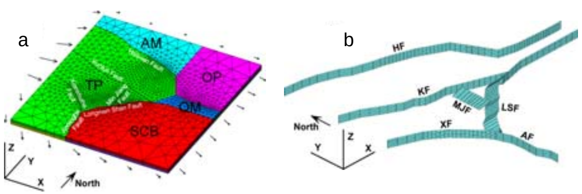

Fig. 2. (a) Mesh and boundary conditions of the finite element model. (b) Mesh of fault systems in the model.

- Model Rheology: 20-km thick elastoplastic upper crust; 20-km thick viscoelastic lower crust.
- Earthquakes are simulated by strain softening of predefined fault elements. Drucker-Prager yield criterion is used.
- Model domain is loaded by velocity boundaries based on GPS data (He et al., 2003 and Zhang et al., 2004) and topography (ETOP30). Top surface is simulated by spring boundary; the bottom is fixed.
- Parallelized codes run on a 16-node dual-core PC cluster.

RESULTS

1. Coseismic slip

We simulate the Mw 7.9 Wenchuan earthquake after the model has reached a quasi steady state. The predicted northeastward unidirectional fault slip, as is observed, can be attributed to the oblique convergence between the Tibetan plateau and the Sichuan Basin on the Longmen Shan fault (LSF). The predicted two separate peaks of coseismic slip on the ruptured LSF, similar to that from seismic inversion (Ji and Hayes, 2008), are related to the bendings of the LSF in the model.

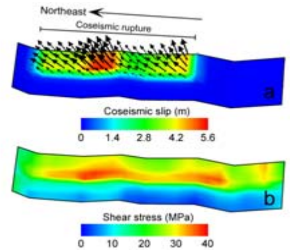

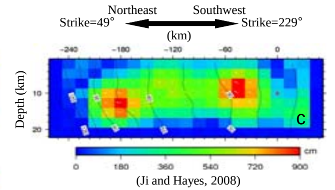

Fig. 3. Model predicted coseismic slip and vector (a), and background shear stress (b) on the bended Longmen Shan fault. (c) Coseismic fault slip from seismic inversion (Ji and Hayes, 2008).

2. Coulomb stress changes by the Wenchuan earthquake

Similar to Parson et al. (2008) and Toda et al. (2008), we found that the Wenchuan earthquake increased the Coulomb stress on southern Xianshuihe fault, the Kunlun fault, northern Min Jiang fault, the Haiyuan fault, and mostly, on the tips of the ruptured LSF (Fig. 4). Continued tectonic loading would fully restore Coulomb stress on the Xianshuihe fault in less than 100 years, but other places of reduced Coulomb stress will remain in the stress shadow (Fig. 5).

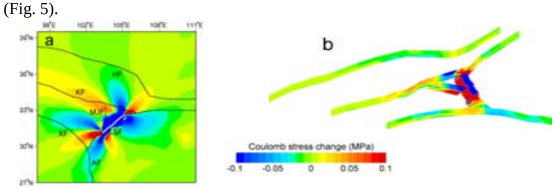

Fig. 4. Predicted coseismic Coulomb stress change on optimal planes in the upper crust (10 km depth) and on major fault systems. Effective frictional coefficient is 0.4. Coulomb stress change is capped by 0.1 MPa.

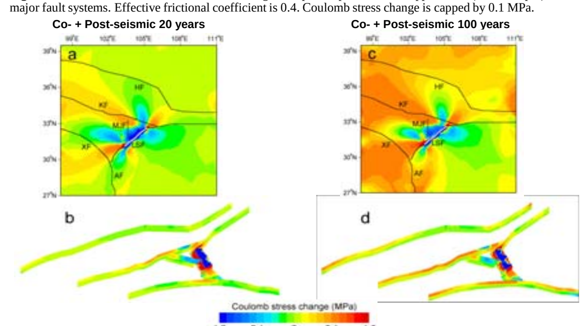

Fig. 5. Predicted Coulomb stress changes 20 years (a-b) and 100 years (c-d) after the Wenchuan earthquake, with postseismic viscous relaxation and continued interseismic loading.

3. Coulomb stress evolution since 1893

We added in the model eight large earthquakes (M≥6.9) in the neighboring region since 1893 and found that the net results are significantly different from that of the Wenchuan earthquake alone (Fig. 6a and 6b). These earlier events have little triggering effects on the LSF except the 1933 Diexi earthquake (Fig. 6c), but their impacts on the hosting faults are much greater than that of the 2008 Wenchuan earthquake (Fig. 6d).

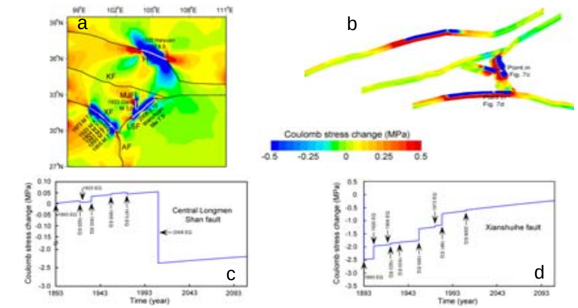

Fig. 6. (a-b) Predicted Coulomb stress changes due to the Wenchuan earthquakes and eight earlier events in the region. (c-d) Coulomb stress evolution since 1893 at the selected points shown in Fig. 6b. Interseismic loading and postseismic viscous relaxation are included. White and gray curves show ruptures by earthquakes.

4. Dynamic fault interactions

To explore dynamic interactions between faults in eastern Tibet, we simulated seismic cycles on the Xianshuihe fault (Fig. 7). We found that when the Xianshuihe fault is locked, the tectonic loading rates on the LFS and other faults are increased (Fig. 8).

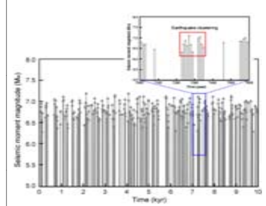

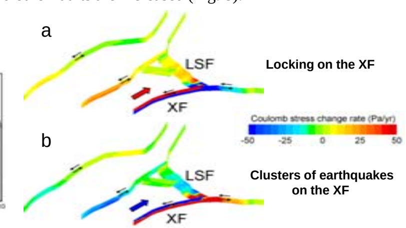

Fig. 7. Simulated seismicity on the Xianshuihe fault. The blowup of selected region shows earthquake clustering.

Fig. 8. The rate of Coulomb stress change (a) when the Xianshuihe fault is locked and (b) when clusters of earthquakes occur on the Xianshuihe fault.

Conclusions

1. The unidirectional propagation of the Longmen Shan rupture during the Wenchuan earthquake is due to the oblique convergence between the Tibetan plateau and the Sichuan Basin.
2. The Wenchuan earthquake increased Coulomb stress on eastern Kunlun fault and southern Xianshuihe fault by up to 0.05 MPa.
3. Except the 1933 Diexi earthquake (M 7.5), previous large earthquakes in eastern Tibet contributed little to the 2008 Wenchuan earthquake. Similarly, the impacts of the Wenchuan earthquake on other faults are overshadowed by the previous events on the hosting faults.
4. Seismicity on the Xianshuihe fault can affect loading rate on the Longmen Shan fault and other faults.